Available online at www.sciencedirect.com

SciVerse ScienceDirect

Ceramics International 38 (2012) 4245–4251

CERAMICS INTERNATIONAL

www.elsevier.com/locate/ceramint

Mechanical behavior of 2.5D (shallow straight-joint) and 3D four-directional braided SiO_{2f}/SiO_2 composites

Yong Liu [a], Jianxun Zhu [a,b,*], Zhaofeng Chen [a], Yun Jiang [b]

[a] College of Material Science and Technology, Nanjing University of Aeronautics and Astronautics, 29#, Jiangjun Road, Nanjing 211106, PR China
[b] Sinoma Science & Technology Co., Ltd., Nanjing 210012, PR China

Received 11 January 2012; accepted 30 January 2012
Available online 9 February 2012

Abstract

The effect of two different fiber architectures on the mechanical properties and mechanical behavior of the SiO_{2f}/SiO_2 composites processed by silicasol-infiltration-sintering has been investigated. The composites were sintered at relatively low temperature (450 °C). The fiber/matrix interface strength was weak. The characteristics of 2.5D (shallow straight-joint) structure and 3D four-directional braided structure were determined. The tensile strength, flexural strength, shear strength and failure mechanisms of both 2.5D (shallow straight-joint) and 3D four-directional braided SiO_{2f}/SiO_2 composites were characterized. It was found that the fiber placement in the preform will strongly affect the mechanical property and failure behavior of the composite. The results of the tests and microstructural observations indicated that 3D four-directional braided SiO_{2f}/SiO_2 composite had better mechanical properties than 2.5D (shallow straight-joint) SiO_{2f}/SiO_2 composite. 3D four-directional braided SiO_{2f}/SiO_2 composite exhibited more graceful failure under loading than 2.5D (shallow straight-joint) SiO_{2f}/SiO_2 composite.

Keywords: B. Composites; B. Microstructure; C. Mechanical properties; Fracture behavior

1. Introduction

Amorphous silica is widely used in a variety of industrial applications due to its high melting point, high thermal shock resistance, and excellent thermal as well as electrical insulating properties. Furthermore, silica is a desirable electromagnetic material because of its low dielectric constant and low loss tangents [1–3]. Unfortunately, due to the low strength and extremely low fracture toughness of the silica in the monolithic form, the use of silica as a structure material is limited [1–4]. However, incorporating fiber preform in the silica composites is a good alternative to silica bulk structure material [2,5]. High-purity quartz fiber with excellent thermal shock damage resistance and dielectric properties is considered the most attractive candidate fiber reinforcement in the silica composite. Previous work mainly concentrated in incorporating short, unidirectional and/or two-dimensional (2D) silica fiber into the silica matrix. It was showed that the fracture work and the mechanical properties were enhanced. However, there is uneven distribution of fibers density in the short silica fibers reinforced silica composites and poor delamination resistance in the 2D silica composites.

More recently, composites reinforced with 2.5D fiber preforms or 3D braided fiber preforms were studied [6–9]. It was shown that their delamination resistance and interlaminar fracture toughness superior to that of the conventional laminated composites. Both of 2.5D weave technique and 3D braided technique can be used to fabricate complex net or near-net shaped components. Furthermore, the properties of the 2.5D composites and 3D composites can be tailored because of the flexibility in fiber placement and fiber hybridization. However, limited attention has been focused toward 2.5D and 3D braided quartz fibers reinforced silica (SiO_{2f}/SiO_2) composites.

As is well known, the fiber architecture is an important parameter which will significantly affect mechanical properties and mechanical behavior of the composites. In order to utilize textile reinforcement structures and SiO_{2f}/SiO_2 composites

* Corresponding author at: Nanjing University of Aeronautics and Astronautics, College of Material Science and Technology, 29#, Jiangjun Road, Nanjing, PR China; Sinoma Science & Technology Co., Ltd., Nanjing, PR China. Tel.: +86 25 52112909; fax: +86 25 52112626.
E-mail address: jianxun_zhu@163.com (J. Zhu).

0272-8842/$36.00
doi:10.1016/j.ceramint.2012.01.083

most efficiently, thorough understanding of their mechanical properties and mechanical behavior are essential. In this paper, 2.5D (shallow straight-joint) preform and 3D four-directional braided preform were used as the fiber reinforcements. The SiO_{2f}/SiO_2 composites were prepared by silicasol-infiltration-sintering (SIS) method. The aims of the current contribution were to compare the mechanical properties and investigate the difference of the mechanical behavior between 2.5D (shallow straight-joint) SiO_{2f}/SiO_2 composites and 3D four-directional braided SiO_{2f}/SiO_2 composites, as well as to expand the experimental knowledge for how fiber architectures impact mechanical properties and mechanical behavior.

2. Experimental details

2.1. Composite preparation

The 2.5D (shallow straight-joint) preforms and 3D four-directional braided preforms were provided by Nanjing Institute of Glass Fiber. The fiber volume fraction of 2.5D (shallow straight-joint) preform and 3D four-directional braided preform were 47.5% and 46.8%, respectively. The SiO_{2f}/SiO_2 composite were prepared by SIS method, the sintering temperature of the composites was relatively low (450 °C) compared with other papers [2,5,10]. The preparation process had been described previously in full detail [11].

2.2. Mechanical properties measurement

Each of the composites provided two types of test specimens. For 2.5D (shallow straight-joint) composite, the specimens were parallel to the warp or weft direction. For 3D four-directional braided composite, the specimens were parallel to the braiding direction or normal to the braiding direction. The as-fabricated 2.5D (shallow straight-joint) and 3D four-directional braided SiO_{2f}/SiO_2 composite were cut parallel to the warp direction and the braiding direction, respectively. Mechanical properties of the composites were characterized under tensile loading, flexural loading and shear loading. Mechanical tests were performed on a pc-controlled electronic universal testing machine (Model CMT5105, SANS Corp., China). Tensile test specimens with dimensions of 3.5 mm × 23 mm × 94 mm were cut from the fabricated composite plates and tapered aluminum tabs were glued at both sides to provide a gauge length of 48 mm. Tensile tests were performed at a constant cross-head speed of 0.3 mm/min. Flexural strength was measured using the three-point-bending method. The nominal flexural specimen dimensions were 3.5 mm × 5 mm in cross section and 40 mm in length. The bending support span size was 30 mm and the crosshead speed was 0.03 mm/min. Shear strength was measured using the Iosipescu shear testing method, meanwhile, the composite panels were cut into two 45° Notched (5 mm depth) beam specimens. The nominal shear specimen dimensions were

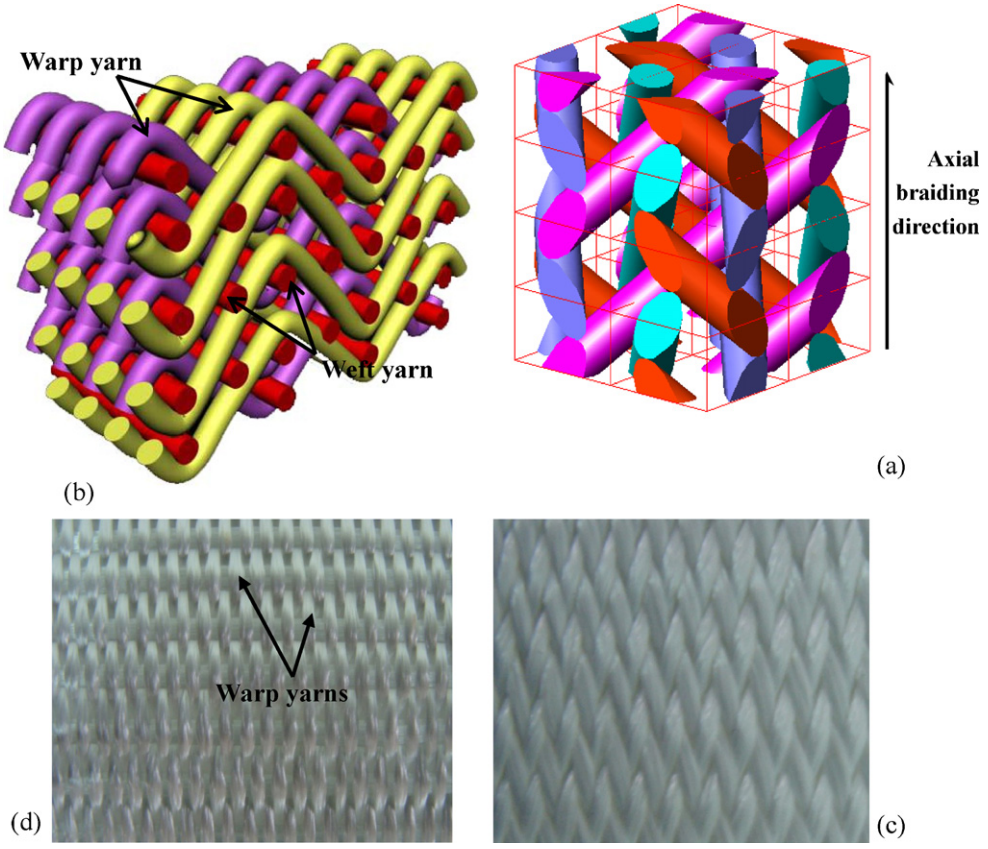

Fig. 1. structures of 2.5D (shallow bend-joint) preform and 3D four-directional preform. (a) Schematic of 2.5D (shallow straight-joint) preform. (b) Schematic of 3D four-directional preform (representative unit cell). (c) 2.5D (shallow straight-joint) preform. (d) 3D four-directional preform.

4 mm × 18 mm in cross section and 80 mm in length. The geometry shear specimens and the test fixture of Iosipescu shear testing method were displayed in the previous literature [11].

2.3. Microstructure observation

The Archimedes technique was used to determine specimen density. The microstructure of the fracture surface was observed by scanning electron microscopy (SEM, FEI CO., Quanta200 and JSM-6360LV). Before observing, the samples were coated with gold (thicknesses of 10 nm) on the surface because the SiO_{2f}/SiO_2 composites were non-conducting samples.

3. Results and discussion

3.1. Preform structure

Fig. 1 shows the structures of 2.5D (shallow straight-joint) preform and 3D four-directional braided preform. 2.5D preform was a unique kind of multilayer fabric. The first set of tows that ran in the weaving direction was called warp yarns, while the second set of tows that ran transverse to the weaving direction was called weft yarns. The 2.5D preform was composed of layers of straight weft yarns and a set of sinusoidal warp yarns, with the adjacent layers of weft yarns interlaced together by warp yarns. The warp yarns were placed at an angle θ, called the undulation angle (see Fig. 1(a)). The warp density and the weft density of the as-received 2.5D preform were 10 picks/cm and 4 picks/cm, respectively. The 2.5D process could produce near-net-shape preforms for components having complicated geometry and thus reduces the production time and associated costs. Especially, this kind of structure could be used to prepare dome-shaped components. Fig. 1(b) shows the representative unit cell of the 3D four-directional braided preform. 3D four-directional braided preforms are composed of four directional yarns which are braided with the same braid angles (interior braiding angle) in the interior of the material. The yarns are solidly interlaced with each other in the space and arrayed in a beeline interiorly (Fig. 1(d)). 3D braided preforms as reinforcements have a number of advantages over conventional laminate preforms, including through-thickness reinforcement, low delamination tendency, high damage tolerance and near-net-shape manufacturing [12].

3.2. Tensile loading

The density of the 2.5D (shallow straight-joint) SiO_{2f}/SiO_2 composite and 3D four-directional braided SiO_{2f}/SiO_2 composite was 1.70 g/cm^3 and 1.71 g/cm^3, respectively. Fig. 2 shows the tensile stress–strain curves of 2.5D and 3D SiO_{2f}/SiO_2 composite obtained by monotonic tensile tests. The curve (a) and the curve (b) show the test results of 3D four-directional braided specimen and 2.5D (shallow straight-joint) specimen. Both of the curves exhibited highly nonlinear behavior. In general, the curves can be divided into four stages (see curve (a)): a very small initial linear stage followed by a large nonlinear stage, and then a quasi-linear stage, and the final fracture stage [13]. At the stage II, because of the increased stress, multiple matrix cracks were generated and the braiding fibers were shear debonded from the matrix. At the stage III, the crack density saturated and the bridging fibers became completely debonded. The stage III was attributed to the elastic response of the bridging fibers. However, different from 3D four-directional braided SiO_{2f}/SiO_2 composite, 2.5D (shallow straight-joint) SiO_{2f}/SiO_2 composite exhibited a large nearly linear-elastic behavior in stage III (Fig. 2(curve (b)). The expected causes were: the additional matrix cracking reached saturation early, and then the bridging fibers fracture appeared to be the dominant damage mode. The average values of the tensile strength for 2.5D (shallow straight-joint) specimen and 3D four-directional braided specimen were 24.5 MPa and 30.8 MPa, respectively. The average values of failure strain for 2.5D (shallow straight-joint) specimen and 3D four-directional braided specimen were 0.75% and 0.56%, respectively. The failure strain of the 2.5D (shallow straight-joint) SiO_{2f}/SiO_2 composite was higher than that of the 3D four-directional braided SiO_{2f}/SiO_2 composite. The reason for 2.5D (shallow straight-joint) SiO_{2f}/SiO_2 composite exhibited high strain was: the warp yarns of 2.5D (shallow straight-joint) SiO_{2f}/SiO_2 composite were placed at an angle θ, these warp yarns exhibited a tendency of parallel to the loading direction when subjected to a tensile load.

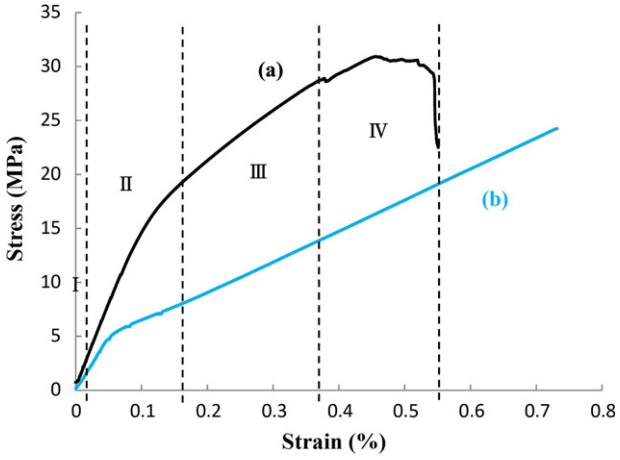

Fig. 2. Comparison of the tensile stress–strain curves for 2.5D and 3D composites (a) 3D four-directional braided specimen. (b) 2.5D (shallow straight-joint) specimen.

3.3. Flexural loading

Fig. 3 shows the stress–deflection curves tested by three-point bending, which were different from that of monolithic ceramics. Toughening effect of quartz preform was obvious. The curve (a) and the curve (b) show the test results of 2.5D (shallow straight-joint) specimen and 3D four-directional braided specimen, respectively. Both of the composites exhibited a non-catastrophic load–deflection behavior. The stress–deflection curves could be divided into three stages: initially linear elastic region, a nonlinear region and final

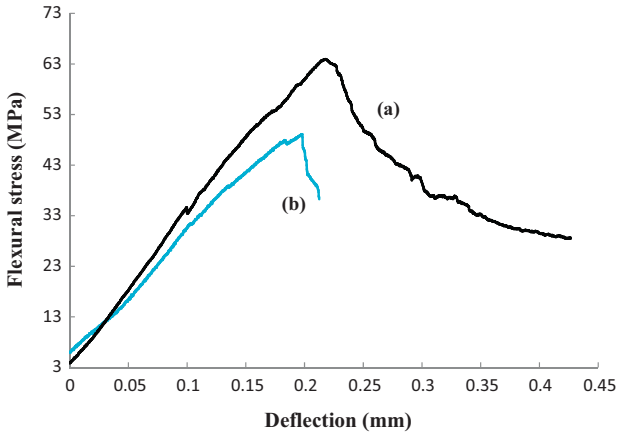

Fig. 3. Comparison of the flexural stress–deflection curves between the 2.5D and 3D composites. (a) 3D four-directional specimen. (b) 2.5D (shallow straight-joint) specimen.

unstable fracture. These three stages had been discussed in full detail in literature [11,14]. As show in Fig. 3, 3D four-directional braided composite exhibited considerable deformation after the maximum load was reached; however, 2.5D (shallow straight-joint) composite exhibited little deformation. The areas under the stress–deflection curve represent the amount of energy that the composite can absorb during the failure process, the size of the area can reflect a certain degree of fracture toughness [15]. The 3D four-directional braided SiO_{2f}/SiO_2 composite absorbed more energy prior to final failure than that of the 2.5D (shallow straight-joint) SiO_{2f}/SiO_2 composite. The average values of the flexural strength for 3D four-directional braided specimen and 2.5D (shallow straight-joint) specimen were 64.0 MPa and 48.4 MPa, respectively.

3.4. Shear loading

The shear strength of the SiO_{2f}/SiO_2 composites was measured by the Iosipescu shear testing method. The loading rate was 0.3 mm/min. Shear strength was calculated by the following equation:

$$\tau = \frac{P}{h\omega} \quad (1)$$

where P is the maximum fracture load (N), h and ω are the height and the minimum distance between v-notched of the sample, respectively.

In general, CFCCs mainly have three kinds of failure modes in the Iosipescu shear testing (Fig. 4(a–c)) [16]. If the reinforcing fibers were perpendicular to the shear loading direction, the failure mode occurs mainly by fiber slipping and debonding at the fiber/matrix interface (Fig. 4(a)). If the reinforcing fibers parallel to the shear loading direction, the failure mode may occur by an interlaminar crack at the sample gage length (Fig. 4(b)). If the CFCCs were reinforced by multidirectional fiber reinforcement (e.g. plain weave fabric), the failure mode may occur by a mixed failure mechanism: besides fiber/matrix interface slipping and interlaminar shear, associated with the fiber bundle splitting in the fabric mesh

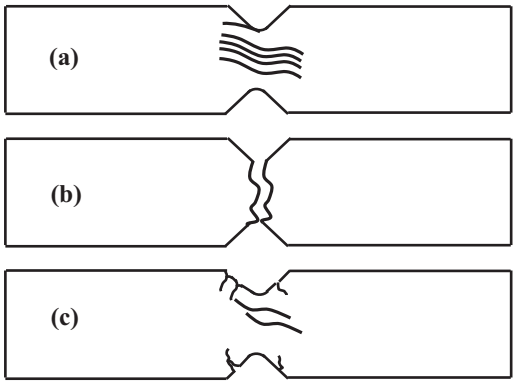

Fig. 4. Modes of failure in the Iosipescu shear testing.

(Fig. 4(c)). As it may, shear properties are mainly influenced by the matrix and the fiber/matrix interface and the shear failure modes are associated with a shear deformation mechanism. Fig. 5 shows the stress–displacement curves of the shear failure behavior of the composites. The curve (a) and the curve (b) show the test results of 3D four-directional braided specimen and 2.5D (shallow straight-joint) specimen, respectively. Both of the curves exhibited mostly nonlinear behavior. The shear failure behavior was similar to the behavior of bending failure. Both types of the composites exhibited a non-catastrophic fracture behavior. Fig. 6(a and b) shows the photograph of the tested Iosipescu specimen of 3D and 2.5D composite, respectively. The fracture surface of 3D four-directional braided SiO_{2f}/SiO_2 composite (see Fig. 6(a)) exhibited a curved fracture path and rugged fracture morphology because 3D braided fiber reinforcement was a multidirectional structure (see Fig. 1(b)). The failure mode of the 3D four-directional braided SiO_{2f}/SiO_2 composites in the Iosipescu shear testing was a mixed mechanism (mode C in Fig. 4). However, the fracture surface of 2.5D (shallow straight-joint) SiO_{2f}/SiO_2 composite (see Fig. 6(b)) exhibited a straight fracture path. Although 2.5D (shallow straight-joint) is a multidirectional structure, the warp yarns and the weft yarns are relatively independent (see Fig. 1(a)). The weft yarns parallel to the shear

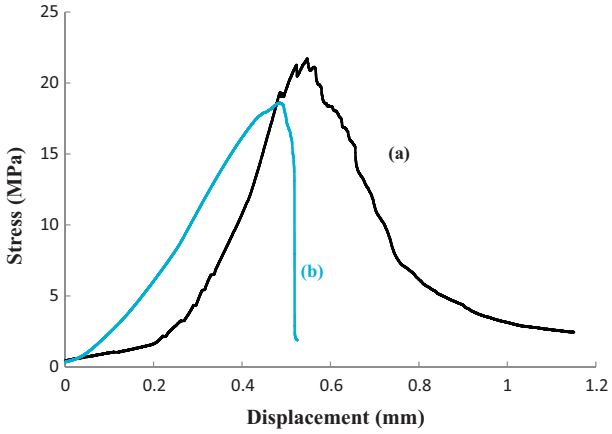

Fig. 5. Comparison of the shear stress–displacement curves between the 2.5D and 3D SiO_{2f}/SiO_2 composites. (a) 3D four-directional braided composite. (b) 2.5D (shallow straight-joint) composite.

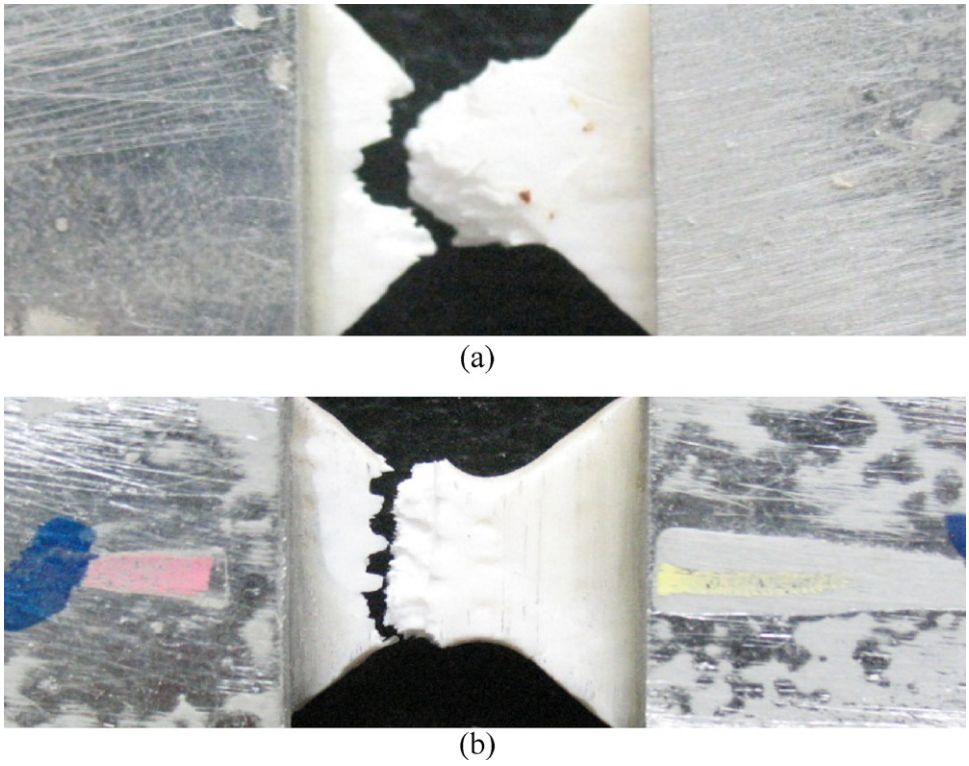

Fig. 6. Photograph of the tested Iosipescu specimen of 3D and 2.5D composite. (a) 3D four-directional braided specimen. (b) 2.5D (shallow straight-joint) specimen.

loading direction, the failure mode of the 2.5D (shallow straight-joint) SiO_{2f}/SiO_2 composites in the Iosipescu shear testing was mode b in Fig. 4. The average values of the shear strength for 3D four-directional braided specimen and 2.5D (shallow straight-joint) specimen were 22.0 MPa and 18.0 MPa, respectively.

4. Discussion

The difference of fiber volume fraction between these two types of composites was very small; however, there were large differences in mechanical properties and mechanical behavior between these two types of composites. The above results clearly indicated that the tensile strength, flexural strength, shear strength and impact energy-absorbing capability of the 3D four-directional braided SiO_{2f}/SiO_2 composite was superior to that of 2.5D (shallow straight-joint) SiO_{2f}/SiO_2 composite. Obviously, the effect of fiber placement affects the failure behavior and toughening mechanisms of the composites. From Figs. 2, 3 and 5, 3D four-directional braided SiO_{2f}/SiO_2 composite exhibited more graceful failure under loading than 2.5D (shallow straight-joint) SiO_{2f}/SiO_2 composite.

Although both constituents (quartz fibers and silica matrix) of SiO_{2f}/SiO_2 composites were brittle, the composites displayed quasi-ductile deformation. The properties of CFCCs were markedly influenced by the interfacial properties. It was generally accepted that interfacial debonding at the fiber/matrix interface was the precondition for crack energy dissipating mechanisms, such as crack deflection, crack bridging, and fiber pull-out [17]. Thus, the interface strength must be weak enough to facilitate the crack energy dissipating mechanisms. There are two main types of bonding at an interface: mechanical bonding or chemical bonding. Mechanical bonding results from thermally induced residual stresses, while chemical bonding arises from chemical reaction during processing. In this study, the composites were prepared at a low temperature, the residual stresses of the composites was relative low. In addition, the strong chemical reactions between the constituents or detrimental change in the fiber preform had been avoided. The interface strength was weak and hence debonding at the fiber/matrix interface was easily achieved under low mechanical load (Fig. 7(a)).

Microscopic observation of the specimens fractured in flexure indicated that both types of composites failed at the tensile side, and no delamination was found for either type of composite. It was found that the yarns were fractured at various regions and the fracture surfaces of the yarns were very ragged. The fracture surface of 3D four-directional braided SiO_{2f}/SiO_2 composite was more ragged than that of 2.5D (shallow straight-joint) composite. For both types of composites, the fibers exhibited multi-step fracture (see Fig. 7(b and c)). From Fig. 7, some fiber pull-out was observed on the fracture surfaces for both types of composites. However, the pull-out lengths of fibers of 3D four-directional braided SiO_{2f}/SiO_2 composite was longer than that of 2.5D (shallow straight-joint) composite; the number of pull-out fibers of 3D four-directional braided composite is more than that of 2.5D (shallow straight-joint) composite. Fiber pull-out was a toughening process operating in the CFCCs during failure. So these two types of composites exhibited a certain degree of toughness. The fracture toughness

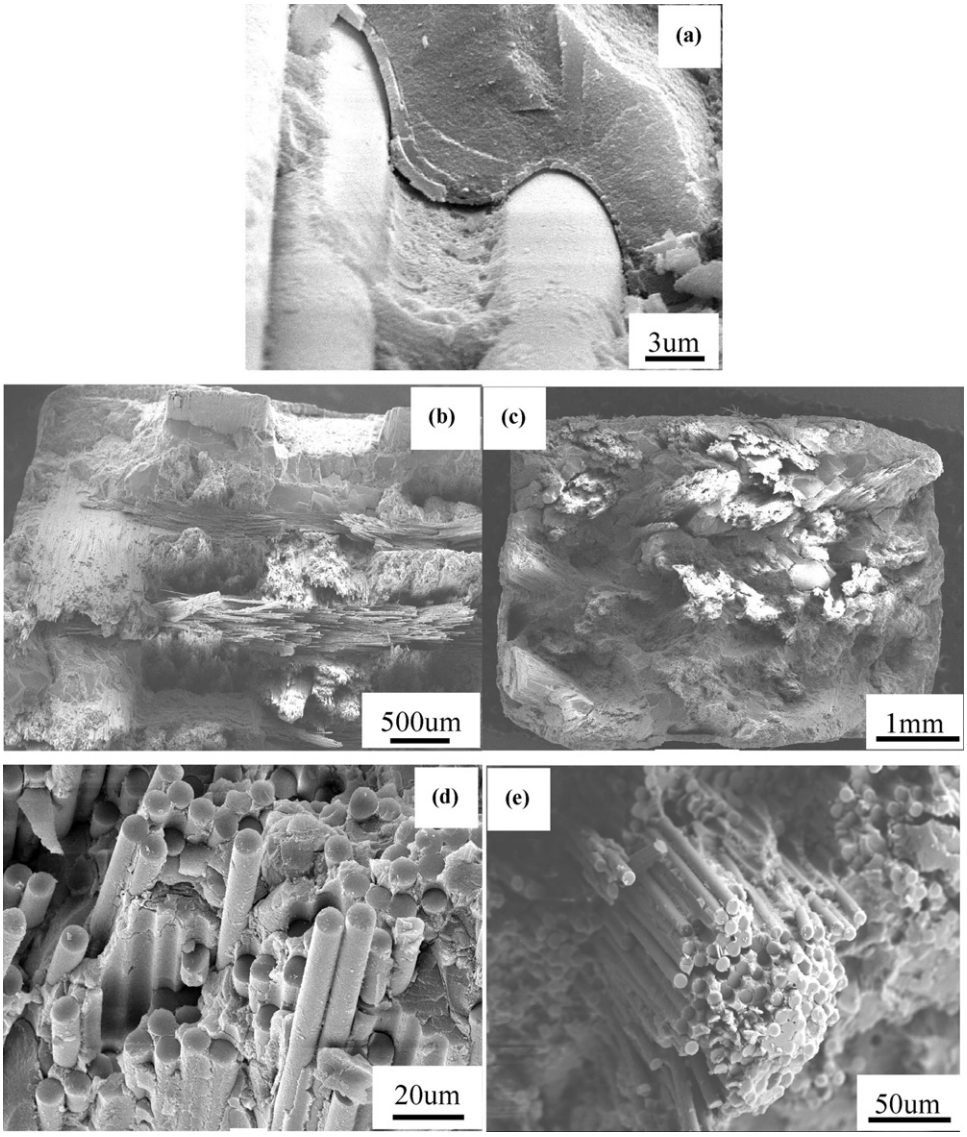

Fig. 7. SEM micrographs of fracture surface of the SiO_{2f}/SiO_2 composites after flexural loading. (a) Interfacial debonding. (b) Fracture surface (2.5D composite). (c) Fracture surface (3D composite). (d) Fiber pull-out (2.5D composite). (e) Fiber pull-out (3D composite).

of 3D four-directional braided SiO_{2f}/SiO_2 composites was superior to 2.5D (shallow straight-joint) SiO_{2f}/SiO_2 composites, this behavior could be more clarified from the flexural stress–deflection curves as shown in Fig. 3.

5. Conclusions

(1) 3D four-directional braided SiO_{2f}/SiO_2 composite had a higher tensile strength, flexural strength and shear strength than 2.5D (shallow straight-joint) SiO_{2f}/SiO_2 composite.
(2) The fiber placement in the preform strongly affects the mechanical property and failure behavior of the composite. The failure modes in the Iosipescu shear testing of these two kinds of SiO_{2f}/SiO_2 composite were distinctly different. 3D four-directional braided SiO_{2f}/SiO_2 composite had a better fracture toughness than 2.5D (shallow straight-joint) SiO_{2f}/SiO_2 composite. Compared with 2.5D (shallow straight-joint) SiO_{2f}/SiO_2 composite, 3D four-directional braided SiO_{2f}/SiO_2 composite exhibited more graceful failure under loading.

Acknowledgments

This work was supported by the Basic Research Project of Science and Technology of Jiangsu Province (No. BK2009002) and Funding of Jiangsu Innovation Program for Graduate Education (No. CXLX11_0188).

References

[1] N.E. Prasad, S. Kumari, S.V. Kamat, M. Vijayakumar, G. Malakondaiah, Fracture behaviour of 2D-weaved, silica–silica continuous fibre-reinforced, ceramic–matrix composites (CFCCs), Eng. Fract. Mech. 71 (18) (2004) 2589–2605.
[2] C.-M. Xu, S.W. Wang, X.X. Huang, J.K. Guo, Processing and properties of unidirectional SiO_{2f}/SiO_2 composites, Ceram. Int. 33 (4) (2007) 669–673.

[3] N.E. Prasad, D. Loidl, M. Vijaykumar, K. Kromp, Elastic properties of silica–silica continuous fibre-reinforced, ceramic matrix composites, Scripta Mater. 50 (8) (2004) 1121–1126.
[4] M.B. Ruggles-Wrenn, P. Koutsoukos, S.S. Baek, Effects of environment on creep behavior of two oxide/oxide ceramic–matrix composites at 1200 degrees C, J. Mater. Sci. 43 (20) (2008) 6734–6746.
[5] H. Chen, L.M. Zhang, G.Y. Jia, W.H. Luo, S. Yu, The preparation and characterization of 3D-silica fiber reinforced silica composites, Key Eng. Mater. 249 (2003) 159–162.
[6] J.Q. Ma, Y.D. Xu, L.T. Zhang, L.F. Cheng, J.J. Nie, N. Dong, Microstructure characterization and tensile behavior of 2.5D C/SiC composites fabricated by chemical vapor infiltration, Scripta Mater. 54 (11) (2006) 1967–1971.
[7] N. Jekabsons, J. Varna, Micromechanics of damage accumulation in a 2.5D woven C-fiber/SiC ceramic composite, Mech. Compos. Mater. 37 (4) (2001) 289–298.
[8] G.D. Fang, J. Liang, B.L. Wang, Progressive damage and nonlinear analysis of 3D four-directional braided composites under unidirectional tension, Compos. Struct. 89 (1) (2009) 126–133.
[9] X.L. Liao, H.J. Li, W.F. Xu, K.Z. Li, Effects of tensile fatigue loads on flexural behavior of 3D braided C/C composites, Compos. Sci. Technol. 68 (2) (2008) 333–336.
[10] S.A. Han, K.H. Jiang, J.W. Tang, Studies on preparation and property of 2.5D SiO(2f)/SiO(2) composites, Adv. Mater. Res. 79–82 (2009) 1767–1770.
[11] Y. Liu, J. Zhu, Z. Chen, Y. Jiang, C. Li, B. Li, L. Lin, T. Guan, Z. Chen, Mechanical properties and microstructure of 2.5D (shallow straight-joint) quartz fibers-reinforced silica composites by silicasol-infiltration-sintering, Ceram. Int. 38 (1) (2012) 795–800.
[12] L. Chen, X.M. Tao, C.L. Choy, On the microstructure of three-dimensional braided preforms, Compos. Sci. Technol. 59 (3) (1999) 391–404.
[13] G. Corman, K. Luthra, in: N.P. Bansal (Ed.), Silicon Melt Infiltrated Ceramic Composites (HiPerComp^{TM}) Handbook of Ceramic Composites, Springer US, 2005, pp. 99–115.
[14] K.G. Dassios, C. Galiotis, V. Kostopoujos, M. Steen, Direct in situ measurements of bridging stresses in CFCCs, Acta Mater. 51 (18) (2003) 5359–5373.
[15] J.M. Yang, W. Lin, C.J. Shih, W. Kai, S.M. Jeng, C.V. Burkland, Mechanical behaviour of chemical vapour infiltration-processed two- and three-dimensional nicalon/SiC composites, J. Mater. Sci. 26 (11) (1991) 2954–2960.
[16] I.V.P. Yoshida, S.R.D.O. Pina, L.C. Pardini, Carbon fiber/ceramic matrix composites: processing, oxidation and mechanical properties, J. Mater. Sci. 42 (12) (2007) 4245–4253.
[17] R.R. Naslain, The design of the fibre-matrix interfacial zone in ceramic matrix composites, Composites Part A 29 (9–10) (1998) 1145–1155.